FIELD ROBOTS

High-resolution outdoor videography of insects using Fast Lock-On tracking

T. Thang Vo-Doan[1]†, Victor V. Titov[1], Michael J. M. Harrap[1], Stephan Lochner[1], Andrew D. Straw[1,2]*

Insects have important roles globally in ecology, economy, and health, yet our understanding of their behavior remains limited. Bees, for example, use vision and a tiny brain to find flowers and return home, but understanding how they perform these impressive tasks has been hampered by limitations in recording technology. Here, we present Fast Lock-On (FLO) tracking. This method moves an image sensor to remain focused on a retroreflective marker affixed to an insect. Using paraxial infrared illumination, simple image processing can localize the sensor location of the insect in a few milliseconds. When coupled with a feedback system to steer a high-magnification optical system to remain focused on the insect, a high–spatiotemporal resolution trajectory can be gathered over a large region. As the basis for several robotic systems, we show that FLO is a versatile idea that can be used in combination with other components. We demonstrate that the optical path can be split and used for recording high-speed video. Furthermore, by flying an FLO system on a quadcopter drone, we track a flying honey bee and anticipate tracking insects in the wild over kilometer scales. Such systems have the capability to provide higher-resolution information about insects behaving in natural environments and as such will be helpful in revealing the biomechanical and neuroethological mechanisms used by insects in natural settings.

INTRODUCTION

Insects, particularly pollinators like bees, are crucial for ecosystem stability and food security through their role in pollination, which is essential for the reproduction of many plants, including numerous crops, and the sustainability of our global food supply (*1*). Like other insect groups, many wild bee species are now suffering marked losses in abundance, likely because of several factors (*2*). Studying insect behavior is an important step in revealing the drivers of these losses and their mechanisms of action. Classically, such behavioral research has been done by direct observation. This has revealed, for example, the waggle dance by which forager bees communicate to naïve nestmates the direction and distance to food sources (*3*). More recently, radar tracking of insects has been developed (*4*, *5*) and used, for example, to study the development of kilometer-scale flight trajectories over the lifetime of a bee (*6*). Despite unique capabilities to track over landscape scales, radar suffers from limited resolution in the spatial and temporal domains (Fig. 1A). To obtain more numerous and higher-resolution data, researchers have built sophisticated laboratory setups with high-resolution cameras in a smaller volume. These cameras have revealed, for example, the biomechanical and sensory basis for decisions made in flight (*7*, *8*), but, because they are in a laboratory, they cannot be used to study insects in their natural environments, where many additional factors may influence performance.

Videography of flying insects has been an important methodology to quantify their behavior, but a stationary camera is subject to a fundamental trade-off imposed by the fixed number of pixels (*9*). If a larger volume is to be filmed, then the pixels must capture a wider area and, hence, have lower angular resolution. Although adding more pixels is possible to sidestep the issue, the image of a moving subject also moves on the sensor, thus creating motion blur. A standard method to overcome these challenges has been simply to reduce relative motion between the subject and the camera using a high-magnification objective and continuously adjusting its aim (*10*). Flying insects, however, are difficult to track with the naked eye, and it is nearly impossible to keep a camera aimed at and focused on them without automation. Use of low-latency optical processing has been used for decades in microscopy to track bacteria, paramecia, and roundworms. In these systems, an optical position signal is used to adjust the microscope stage such that the subject remains at the system's focus (*11*–*13*). For an animal or robot moving at larger spatial scales, however, another solution is necessary. For inanimate objects such as sports balls or drones and for larger animals such as birds, high-magnification optics have been combined with high-speed image analysis to enable tracking and videography (*14*–*16*). Tracking insects with such systems, however, remains challenging. Simplifying the complexity of the tracking task to achieve the necessary low latency is essential, and one solution is to use simplified indoor backgrounds (*17*). Another solution is to translate a frame carrying multiple cameras around a flying insect using multiple winches comprising a cable robot within a specially equipped space (*18*).

Affixing an optically distinct marker, such as one that is much brighter than the background or has a unique color, could simplify the image processing task and, hence, make it robust and fast. One choice would be to use a fluorescent or luminescent marker, which works in sunlight (*19*). However, the requirement for sunlight is potentially limiting for studying, for example, nocturnal insects and the effects of artificial light at night. Moreover, omnidirectional emission of fluorescence and luminescence greatly reduces the intensity and, hence, the maximum tracking range of returned light. On the other hand, retroreflectors return most incoming energy to within a small angle of the incident direction and may be suitable as markers when combined with paraxial illumination such as from a light-emitting diode (LED) near the camera lens. Retroreflective markers are widely used in commercial (human) motion-capture systems and have already been used in a variety of insect-tracking tasks (*7*, *20*–*22*).

[1]Institute of Biology I, Faculty of Biology, Albert-Ludwigs-Universität Freiburg, Freiburg, Germany. [2]Bernstein Center Freiburg, Albert-Ludwigs-Universität Freiburg, Freiburg, Germany.
*Corresponding author. Email: straw@bio.uni-freiburg.de
†Present address: School of Mechanical & Mining Engineering, University of Queensland, Brisbane, Australia.

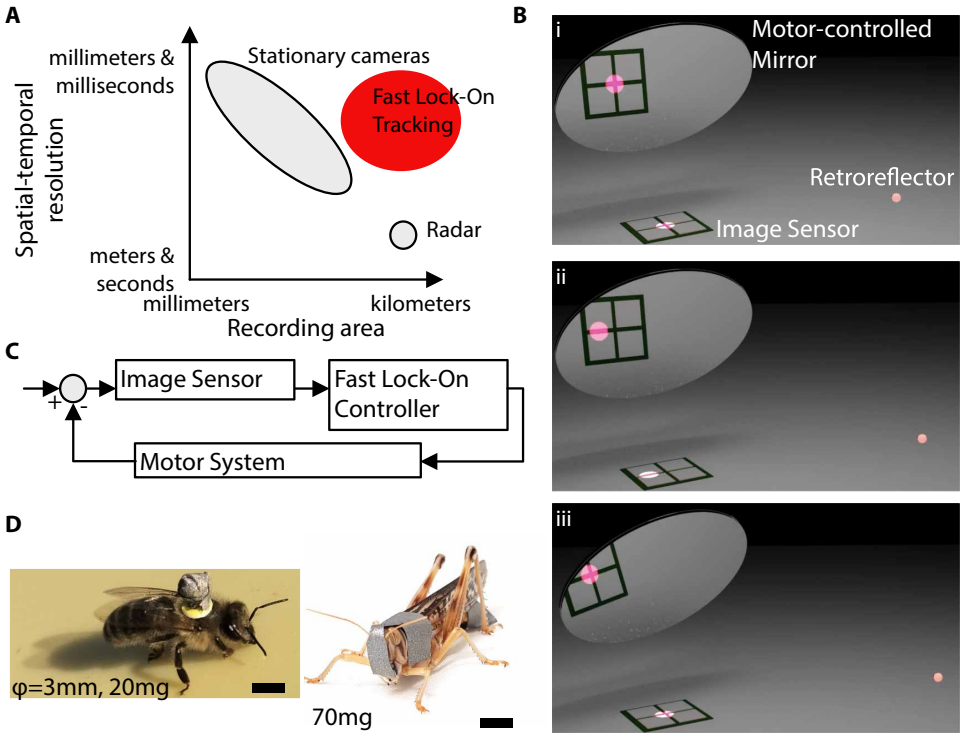

Fig. 1. FLO tracking bypasses trade-offs of other insect tracking techniques. (**A**) Conceptual view of tracking systems based on stationary cameras, radar, and FLO tracking. Moving cameras allow expansion of the recording area beyond stationary cameras, but, without an FLO system, it has not been possible to follow insects with a moving camera because of their small size and speed. (**B**) At the starting configuration (i), the system is aimed such that the image of the insect-mounted reflector is focused in the center of the image sensor. Note that illumination and focusing optics are omitted from the illustration. When the insect moves, the reflected spot is initially offset from the sensor center (ii). On the basis of image processing and motor action, the system automatically adjusts the mirror position to recenter the spot with low latency (iii). (**C**) Schematic block diagram showing that the input to the image sensor is the angular difference between the insect angle and the motor-controlled optical path angle. (**D**) Examples of insects carrying representative retroreflective markers tracked with FLO systems include the honey bee *A. mellifera* (marker diameter, 3 mm; mass, 20 mg; scale bar, 3 mm) and the locust *S. gregaria* (marker mass, 70 mg; scale bar, 3 mm).

Our own preliminary work has been promising (*23*), and, here, we report a full follow-up.

Here, inspired by these earlier works, we implemented what we call Fast Lock-On (FLO) tracking. We applied FLO to the task of tracking insects flying outdoors, which remains an incompletely solved yet important problem. We describe a series of robotic systems, from simple to more sophisticated, exploring the idea of FLO tracking and illustrating their potential for use. In one system, we share the optical path of the FLO-based tracker with a high-magnification, high-speed camera system to make high–spatiotemporal resolution videos of freely flying insects. In another system, an FLO-based tracker mounted on a quadcopter was used to follow a bee over tens of meters.

RESULTS

Implementation of FLO tracking

The basic principle of FLO tracking is to use feedback from an optical sensor to steer its optical axis, for example, by tilting a mirror, in a manner that minimizes deviation of the target image from the center of the sensor (Fig. 1B). The time history of the optical axis position and sensor output can be used to compute the tracked object's trajectory. Low latency from sensor input to motor output will improve system performance and enable higher magnification optics, which, in term, can lead to further performance gains. From a control perspective, FLO is a closed-loop design in which the displacement of the target image from the sensor center is an error angle between the insect angle and the angular position of the optical path under control. The FLO controller sends motor commands to minimize this error and receives feedback through the optical sensor (Fig. 1C). To track insects using FLO systems, we incorporated infrared illumination near the optical axis of the optical sensor and marked the insect with a small, lightweight retroreflective marker (Fig. 1D). This allowed us to reconstruct the flight path of an insect in angular terms as measured from the FLO system.

We implemented a simple FLO system with a handful of inexpensive parts, namely, a low-latency (on the order of 10 ms) digital camera, a pan-tilt motor system, and a computer (Fig. 2 and Mini-FLO in data file S1). Despite being relatively simple, this system was useful as a starting point for more sophisticated hardware and experimenting with different image processing and control algorithms. To reduce the latency of image processing, we implemented only a very simple bright point detector. On the control side, although it is possible to implement FLO tracking with an internal model estimating only the angular error of the target with respect to the moving optical axis and updating motor commands accordingly, we found that using a Kalman filter to estimate both the angular position and velocity of the target with respect to a fixed reference frame improved tracking robustness because the system was then able to maintain tracking during occlusions.

Because FLO tracking views the target through the optical path under control, calibration is simplified compared with that of a system in which a separate camera system is used to steer the optical path for a high-magnification sensor (*24*, *25*). The low-latency, closed-loop performance contributes to improved robustness not only by simply increasing the frequency of disturbances, which can be compensated, but also by minimizing the maximum displacement over time of a moving target and thus reducing the difficulty for a tracking system to distinguish which of multiple potential targets corresponds to the object being tracked. With the use of beam splitters or selective transmission mirrors, "copies" of the optical path can be built and imaged using cameras with different characteristics from those of the tracking camera.

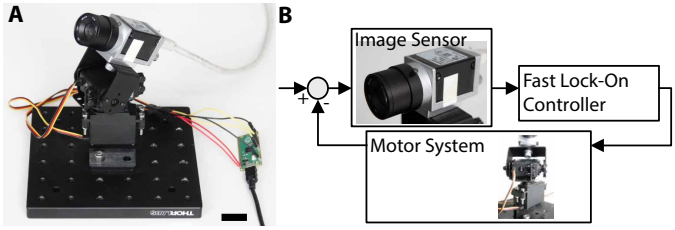

Fig. 2. Simple FLO tracking system. (**A**) For prototyping algorithms and software, a simple pan-tilt system can be built from commercial off-the-shelf parts. Scale bar, 25 mm. (**B**) The system architecture allows gain of experience in FLO tracking.

High-speed, high-resolution videos of insects flying outdoors

To make high-resolution videos of insects flying outdoors, several challenges remain. One challenge is that direct or reflected sunlight can be detected by our simple image processing instead of the insect's attached marker. Therefore, we sought to minimize the recorded brightness of sunlight and maximize the intensity of the retroreflective target image by confining our illumination and detection to the same, narrowly defined temporal and spectral windows. This maximizes the signal recovered from the illumination power but minimizes the noise from sunlight. We used high-power pulsed illumination paired with corresponding short exposure integration times. Spectrally, the infrared emitting diodes were matched to narrowband spectral filters on the cameras.

Another challenge is acquiring video of the insect, rather than a recording of a bright point of light on a dark background. To overcome this challenge, we used a selective transmission mirror to direct the infrared light path to the tracking camera and visible light to a high-speed video camera that could be triggered to record at 1000 or more frames per second. Obtaining sharp, well-illuminated videos with this system, however, requires the use of a long–focal length objective with a large aperture and, consequently, a large-diameter optical path that is redirected to follow the insect. Therefore, we developed a large-size pan-tilt mirror periscope turned by stepper motors with a design goal of minimal mass and, therefore, minimal inertia and thus latency.

A large-aperture, long–focal length objective has a shallow depth of field; thus, a final challenge is maintaining focus on a flying insect. We used a second tracking camera to implement a stereo camera pair. Distance estimates from stereo disparity get less precise with increasing distance, but this decreased distance precision is matched by an increased depth of field at larger distances. We combined these design elements in a single system capable of recording high-speed, high-magnification video of freely flying insects in natural, outdoor settings (Fig. 3).

To validate the FLO-based high-speed, high-resolution video system, we tracked a toy quadcopter to which a retroreflective marker was attached. Testing confirmed that all system components functioned and that high-resolution, high-speed videos could be acquired over a large field of view using a stereo-based autofocus system in an indoor setting (Fig. 3C and movie S1).

We next moved our system outdoors with the goal of recording high-speed, high-resolution video of insects behaving in naturalistic conditions. After marking insects with retroreflective markers, we were able to track them with our FLO system and record videos in which the head-tail length of the insect was hundreds of pixels long with little or no motion blur (Fig. 3D, Movie 1, and movies S2 to S4). The mass of the reflective marker ball attached to the bees was about 20 mg. For *Bombus terrestris* bumble bees, this compares to an average forage load of 47 mg (*26*) and, in *Apis terrestris*, to an average forage load of 17 to 25 mg (*27*). We did not observe any obvious changes in behavior or other effects due to the added mass, aerodynamic changes, or other perturbations caused by our markers.

Accuracy and precision of FLO-based position measurements

To obtain an estimate of the performance of this system in producing three-dimensional (3D) position estimates of the tracked object, we returned indoors, where we acquired a dataset in which the toy quadcopter was tracked with both the FLO system and a conventional motion capture system using stationary cameras (movie S5). In the FLO-based system, the pan and tilt motor positions, together with the disparity measurement from the stereo tracking cameras, were used to compute spherical coordinates that were then converted to Cartesian coordinates. We flew the quadcopter though a space filling an axes-aligned bounding box of 2.3 m by 1.0 m by 1.5 m. The FLO-based system and the stationary camera system showed close agreement in estimated 3D coordinates (Fig. 3E). To obtain a quantitative estimate of absolute tracking accuracy and precision with this FLO system, we affixed retroreflective markers to the ends of a 1500-mm rod (measured with a 5-m tape measure from Duratool) and performed 88 measurements of its length throughout a multiple-meter volume. The rod was held in multiple configurations, such as oriented almost directly away from the FLO system, perpendicularly to the line of sight from the FLO system, and at a variety of positions in the volume. The mean absolute error was 1.96 cm, or 1.3%, and the distribution of errors is shown in Fig. 3F.

Recording bee trajectories from a flying quadcopter drone

Last, we sought to test the feasibility of tracking bees from a flying quadcopter using a lightweight, self-contained FLO system (Fig. 4A). For this system, the image sensor and illumination source were the same as those described in the previous section (Fig. 4B). With this system, we were able to track marked honey bees for several minutes and could measure the pan, tilt, and distance from the drone to the tracked bee. A drone pilot followed the bee with the drone to keep the bee within tracking range of the drone. Data fusion with GPS and attitude data from the drone allowed reconstruction of the 3D trajectory of the bee (Fig. 4, C to E, and Movie 2). With the present system, we anticipate that tracking will be limited to areas where no specular reflections of the LED other than the insect-mounted retroreflector are present.

DISCUSSION

Here, we described FLO tracking and used it to acquire high-speed, high-resolution videos of insects flying outdoors. These videos filmed the insect from takeoff to landing with high magnification and low motion blur. Appendages such as legs, wings, and antennae remained in focus, even as the insects flew. We further demonstrated an FLO system mounted on a quadcopter to track the position of a flying honey bee.

As a methodology, FLO tracking has some drawbacks. Closed-loop tracking requires that an initial lock must be established via a separate process, and, if tracking is lost momentarily, this may result

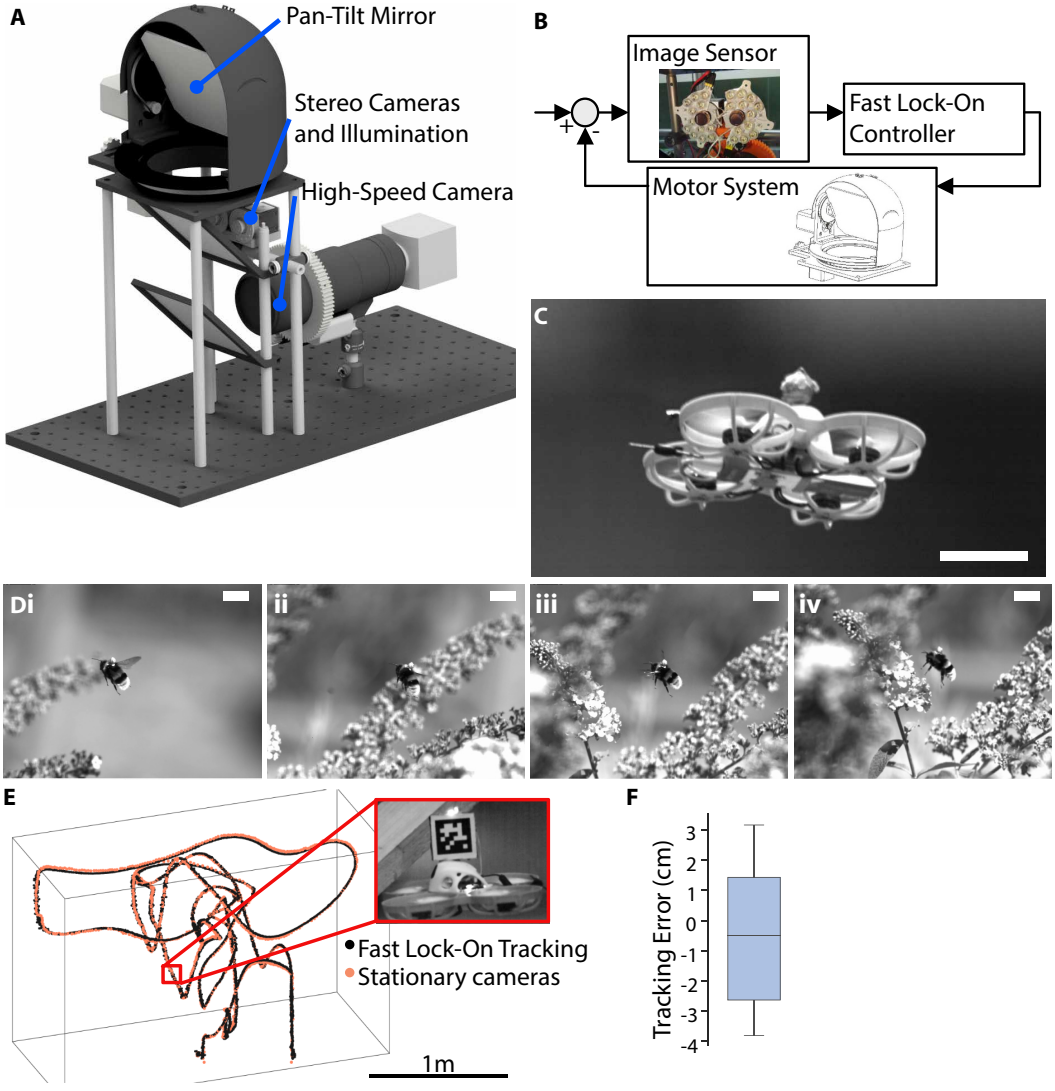

Fig. 3. Large-diameter optical path shared with a high-speed telescopic video camera to record high-resolution insect video during natural behavior. (**A**) A large-diameter optical path is steered by an FLO system incorporating active infrared illumination and a low-latency infrared stereo camera pair. A wavelength-selective mirror allows high-speed videography of the scene along the same optical axis. Stereo disparity is used to control a focus motor on a high-magnification objective. (**B**) The FLO core uses one camera from a stereo camera pair and paraxial infrared illumination to provide feedback about the position of a small retroreflective marker, which is then used to drive a motor pair to reorient the optical axis over a large angular range. (**C**) Example image from a high-speed, high-resolution video of a toy quadcopter. Scale bar, 40 mm. (**D**) Example frames from a high-speed video of a bumble bee landing. Marker size, 3-mm diameter; mass, 20 mg; scale bar, 15 mm. (**E**) Simultaneous 3D tracking with a conventional motion capture system using five high-resolution stationary cameras (orange points) and a single FLO system (black points) over several meters. Inset shows a single frame from a high-speed video of 300 frames per second acquired using a high-speed camera directed with an FLO system. (**F**) Absolute tracking errors were quantified by measuring a 1500-mm-length rod in 12 configurations distributed throughout a multiple-meter tracking volume. The box shows quartiles with the median shown as a line, and whiskers show the entire data range. $n = 88$ measurements.

in a complete loss of tracking. Another drawback is that distance estimation must be performed additionally to the basic FLO concept. Here, we partially overcame this problem with stereopsis to measure distance and adjust focus. Other solutions, such as measuring time of flight of light pulses, are worth investigating as alternatives. Furthermore, although successful tracking does not require careful calibration, extracting final 3D coordinates and estimating their accuracy will require careful calibration.

Computational demands from image processing were minimized using a retroreflective marker in the systems described here. Affixing the mark to an insect, however, requires physically manipulating the insect to be tracked and, although we did not observe any notable examples, it potentially causes interference with behavior. The requirement to use retroreflectors could be lifted if more sophisticated computer vision methods could be developed to perform the required task. It would be worthwhile to investigate the use of marker-free approaches making use of object detectors based on artificial neural networks (*28*) or event cameras (*29*).

Several further improvements are conceivable. The human pilot controlling the drone could be replaced with an FLO-directed

Movie 1. High-speed video of a bumble bee captured using FLO tracking.

autopilot. The use of multiple FLO systems working together would theoretically allow calculation of 3D coordinates and distance estimation via triangulation. These systems could operate independently and the data combined afterward for processing, but, if they would work cooperatively during tracking, then improved robustness to occlusions and larger tracking volume coverage could also be achieved. This would involve calibrating multiple systems in a common frame and implementing higher-level coordination such as sending, receiving, and using estimated positions between individual FLO systems. For the drone-based systems, this could involve using real-time kinematic global navigation satellite system receivers in conjunction with onboard inertial measurement units.

We suggest that FLO tracking could potentially be applied to study the biomechanics of insect landing behavior; to study the orientation of the head and eyes during learning flights of bees; to study the altitude at which bees fly; and to study responses of insects to artificial light at night, pesticide treatment, or habitat loss. All of these research topics have open questions, and progress is presently limited by the technology available for recording insect behavior.

MATERIALS AND METHODS

FLO controller

The closed-loop controller was a standalone executable written in the Rust programming language, which can be compiled for Linux, Windows, and macOS operating systems. The core inner loop updated a Kalman filter where the prediction step consisted of computing the predicted (a priori) state estimate and covariance. The Kalman filter estimated the 4D state $\boldsymbol{x} \equiv \phi, \dot{\phi}, \theta,$ and $\dot{\theta}$ representing the pan angle, pan angular velocity, tilt angle, and tilt angular velocity in a coordinate frame fixed relative to the base of the fast mirrors (the stationary in the world frame except in the case of the drone). Observations for the pan-tilt system were the sensor coordinates provided by the Imops module of Strand Camera software. Ongoing lag-compensated estimates of motor angles were maintained via nonprobabilistic representations empirically fit to motor data. Motor commands were then computed for each cycle through the loop. A standard PC was used to run the controller software. In the case of the drone, to reduce mass, this PC (ASRock 4×4 Box-5800U) was mounted to the drone without its housing.

Angle transformations

To provide the Kalman filter with observations of the target position in global motor angle coordinates ϕ_t (pan) and θ_t (tilt), these coordinates were reconstructed from the current (estimated) motor position ϕ_0, θ_0 and the apparent target position in sensor angle coordinates x and y using the linear approximation

$$\begin{pmatrix} \phi_t \\ \theta_t \end{pmatrix} \approx \begin{pmatrix} \phi_0 \\ \theta_0 \end{pmatrix} + \begin{pmatrix} 1/\cos\theta_0 & 0 \\ 0 & 1 \end{pmatrix} \cdot R(\phi_0) \cdot \begin{pmatrix} x \\ y \end{pmatrix} \quad (1)$$

Depending on the specific system geometry, the image did (moving mirror setup) or did not (moving camera drone setup) pick up the roll angle equivalent to ϕ_0, which is reflected by different choices

$$R(\phi_0) = \begin{pmatrix} \cos\phi_0 & \sin\phi_0 \\ -\sin\phi_0 & \cos\phi_0 \end{pmatrix} \text{(moving mirror)}; \quad R(\phi_0) = \begin{pmatrix} 1 & 0 \\ 0 & 1 \end{pmatrix} \text{(moving camera)} \quad (2)$$

for the two setups.

Cameras, image acquisition, and infrared illumination

Cameras used for low-latency image acquisition were a digital camera capable of 160 uncompressed frames per second in full frame mode and more than 1000 frames per second with a small region of interest (Basler ace 2 a2A1920-160umBAS). For experiments involving stereo images for distance estimation, an external trigger device provided voltage pulses to synchronize acquisition. Image acquisition and low-latency processing was performed with Strand Camera 0.12 (Straw Lab). Image processing was implemented in the Imops module of Strand Camera, which implements single-instruction–multiple-data–accelerated operations to find the location of the brightest pixel. For experiments with the high-speed video camera and the drone, a custom circuit board carrying high-intensity infrared LEDs (SFH 4715AS A01, Osram) was used as an illumination source, and Thorlabs FBH05850-10 band-pass filters were used to cut other sources of illumination. For all systems, a 25-mm focal length objective (IDS-5M12-S2524, IDS Imaging) was used.

For high-speed, high-resolution video, we used a long focal length macro lens (Nikon AF Micro Nikkor 200 mm f/4D) and camera (Mikrotron MotionBlitz EoSens mini1). The motion capture system used to obtain independent 3D measurements of the quadcopter trajectory was Braid 0.12 (Straw Lab) using five Basler ace 2 a2A1920-51gcBAS cameras.

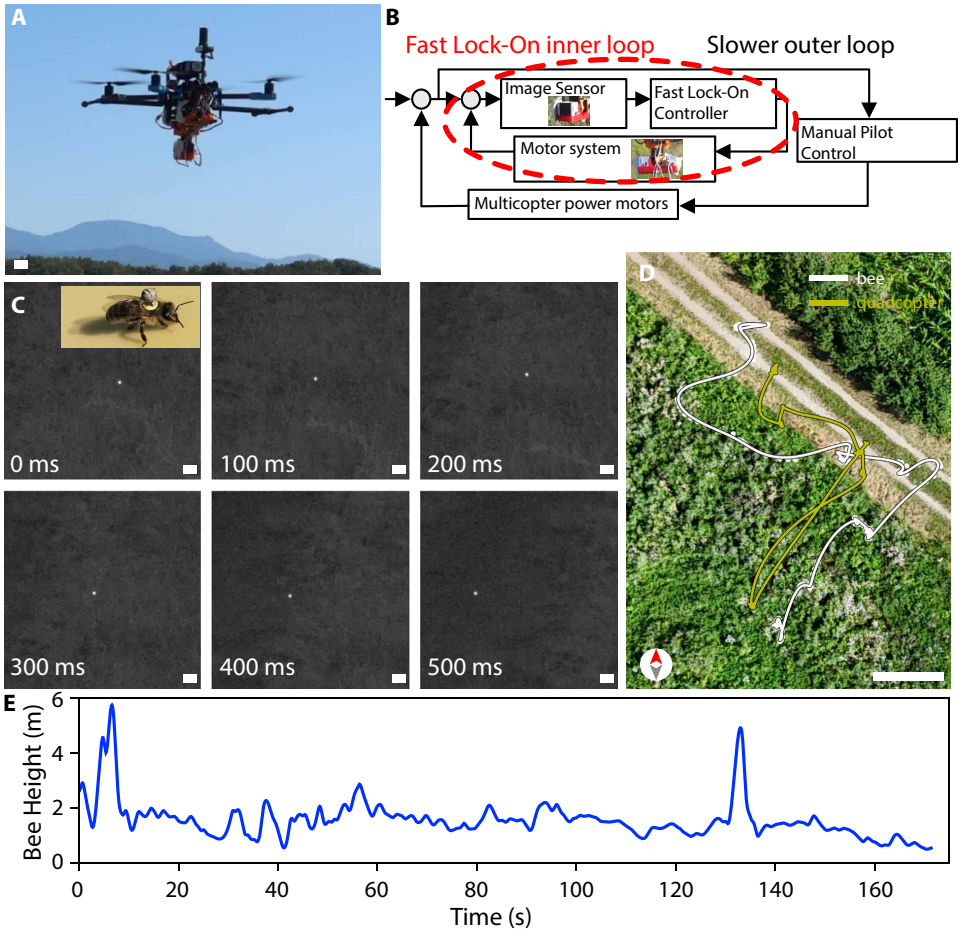

Fig. 4. Quadcopter-mounted FLO system for tracking insects. (**A**) A quadcopter is equipped with an FLO system optimized for low mass. Scale bar, 40 mm. (**B**) The sensor and illumination are a stereo pair of video cameras with paraxial infrared illumination. Images are processed on a PC carried onboard the quadcopter and drive the pan-tilt motor system automatically. Bee angular position information is conveyed to the pilot, who attempts to steer the drone such that it remains within tracking range of the bee. (**C**) Example video frames acquired during tracking of a marked *A. mellifera* honey bee. Scale bars, 20 mm. (**D**) Map of tracked 3D bee position plotted over an aerial photo of the location. Scale bar, 5 m. (**E**) Height of bee aboveground computed during flight shown in (D).

The size of the spot decreases as $1/r$ as the marker is moved farther away from the camera, but that is not an issue until the size gets smaller than 1 pixel (or the diffraction limit of the lens). Beyond that, an additional r^{-2} multiplier will creep in. In other words, the pixel value will now be determined by the total energy received by the camera, not the illuminance at the center of the spot. This falloff (r^{-4}) is extremely fast, so the point where the reflector size corresponds to 1 pixel of the camera can be considered a hard limit for how far the tracking can work. We experimentally verified that pixel values do fall off as r^{-2} when the image of the reflector is much larger than 1 pixel.

It may be useful to consider how to double the tracking distance. First, Φ_{LED} should be quadrupled. Then, to avoid the r^{-4} falloff, either the magnification of the lens could be increased to fill more pixels with the image of the reflector, the size of the reflector could be increased to fill more pixels, or an intermediate combination of the two could be applied. Given that the image of the reflector scales linearly with the reflector radius, the reflector linear dimension should be doubled if the lens magnification is maintained. We note that increasing the magnification may decrease tracking robustness given that it may also result in slower movement and decreased field of view. When considering miniaturizing the reflector, the same considerations apply, and one should choose system components such that the reflector image remains larger than 1 pixel.

Design considerations for active illumination and retroreflectors

The principal requirement is that the brightness of the retroreflector as seen by the camera (pixel value) is higher than the brightest parts of a sunlit environment. If the image of the reflector is larger than 1 pixel in width, then the pixel value is approximated by

$$I_e = A \cdot \Phi_{LED} \theta_{LED}{}^{-2} \theta_{refl}{}^{-2} r^{-2} \quad (3)$$

where I_e is the illuminance of the sensor (pixel value), Φ_{LED} is the output light flux of the LED, θ_{LED} is the angular divergence of the LED beam, θ_{refl} is the angular divergence introduced by the retroreflector, r is the distance to the marker, and the factor A captures the contributions of everything else (constants and unit conversions, losses in LED reflector lens, lens aperture, filter transmission, and retroreflector loss). We assume that the camera lens is focused on the marker, that θ_{LED} and $\theta_{refl} << 1$, that the lens pupil is less than $r \cdot \theta_{refl}$, and that the LED-to-pupil distance is less than $r \cdot \theta_{refl}$.

Motor systems

The mini-FLO system uses hobby servos arranged in a pan-tilt configuration (RB-Lyn-74, Robotshop) onto which the camera is physically mounted. The high-resolution camera system uses smart stepper motors (PD42-2-1240-TMCL, Trinamic). The drone uses brushless gimbal motors (GM2804H-100T Encoder Combo Set, iFlight). The drone itself was a Holybro X500 V2 with a Holybro H-RTK F9P Helical GPS RTK Module.

Reflector marker attachment to desert locusts

Winged adult-stage desert locusts, *Schistocerca gregaria*, were obtained from BUGS-International GmbH (Irsingen, Germany). Locusts were housed in groups of up to eight within a vivarium (30 cm by 30 cm by 40 cm) in laboratories and fed wet green lettuce daily until individuals were removed for testing.

Markers attached to locusts were made of several sections of retroreflective tape (3M Scotchlite 8850 Reflective Material Silver marking film, 3M Company, Maplewood, Minnesota, USA) and

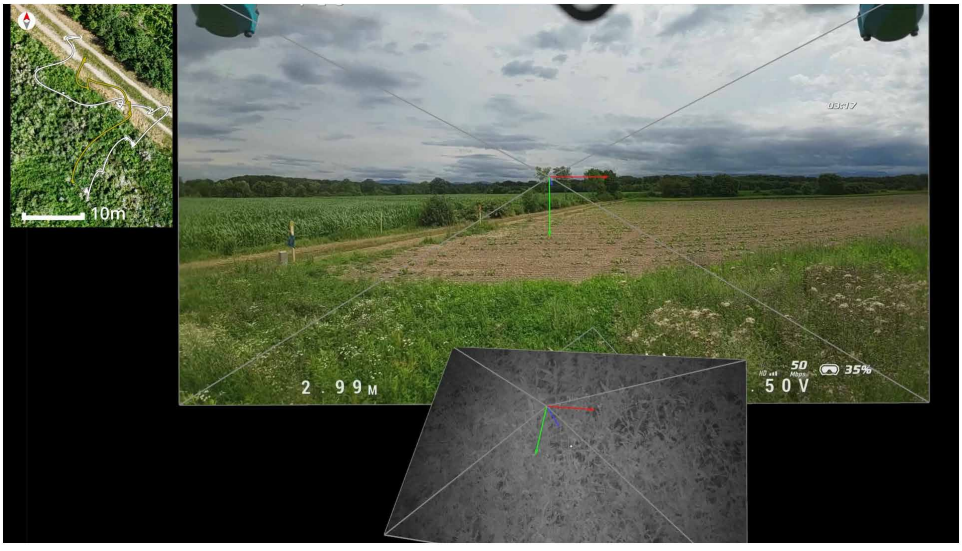

Movie 2. Tracking a bee with a quadcopter-mounted FLO system.

adhered to the insect using the tapes' own adhesive backing (see Fig. 1D). First, a "saddle" or trapezoid-shaped section was applied across the pronotum section of the locust's thorax (~20- and 10-mm wide at the long and short end and 10-mm deep). Care was taken to not apply this section of tape beyond the pronotum. Second, a rectangular section was applied to the front of the insect's head (~2 mm by 5 mm), avoiding the antennae and compound eyes. Third, a rectangular section was applied to the ventral surface of the locust's thorax (~6 mm by 6 mm), with care taken to not restrict movement of the locust's legs. In some trials (as seen in Fig. 1D), a fourth section was applied to the ventral surface of the locust's abdomen (~6 mm by 6 mm).

All sections were cut to size after direct comparison with the insect to be marked. Thus, marker sections varied in exact size and shape (note that all sizes reported above are approximations). Locusts were not anesthetized during attachment of markers. Instead, markers were attached while the insect's hind legs were held across the femurs and abdomen, preventing escape behavior. All sections were applied with nitrile-gloved hands and pressed down further with a blunt-seeker tool. If the marker sections did not adhere easily to the hard sections of the insect's body, then these sections were lightly scraped with an emery file to rough up this surface and facilitate tape adhesion; however, this was rarely required. Collectively, the marker sections applied to the locust weighed, on average, 70 mg (mean) (range of 64 to 76 mg; based on five measurements of tape sections).

Reflector marker attachment to bees

Bumble bee colonies, *B. terrestris*, were obtained from colonies purchased from Biobest (Westerlo, Belgium), and honey bees, *Apis mellifera*, were obtained from hives maintained on site. Honey bee colonies were maintained using standard beekeeping practices by an on-staff beekeeper; however, colonies were kept outside, and bees were otherwise required to forage on local flora for food. Because these bees were raised commercially, no permit for working on wild insects was required.

The markers attached to both bee species were of identical design, and procedures for attachment of markers were also identical for both species. Bee retroreflective markers consisted of a 3-mm retroreflective sphere attached to a queen marking plate (Opaliths, Pasieka, Dolna, Poland) stuck to the bee's back (Fig. 1D). Retroreflective spheres were made as follows: Small 3-mm polystyrene balls (TEDi GmbH & Co. KG, Dortmund, Germany) were wrapped in a 20 mm–by–3 mm strip of retroreflective tape and stretched during application to minimize creasing until the complete surface of the ball was covered. This retroreflective sphere was then stuck directly to the outward face of a queen (bee) marking plate with super glue (Loctite original, Henkel Corporation, Westlake, Ohio, USA). Use of the marking plate as a base of the marker allowed the sphere to be held higher and allowed better and cleaner attachment of the marker to the bee compared with directly sticking the sphere to the bee. Such plates fit the bee thorax and limited the spread of the glue applied beneath them. Markers were prepared, as described above, before bee capture to minimize the time bees spent captive.

Foraging bees from colonies were caught using butterfly nets upon exiting the colony. Bees were not anesthetized for marker attachment; instead, captured bees were transferred to a "queen marking" or "drawing tube" with a net head and foam slider to hold bees in place (Josef Muhr Beekeeping, Prakenbach, Germany). In these devices, bees were positioned and held still against a net grid with the dorsal section of their thorax exposed through the net grid. The dorsal section of the thorax was shaved of hair with a razor blade to allow marker plates to be stuck directly to the bee's cuticle, not its hair, further facilitating adhesion. The marker was then stuck to the bee using the marking plate base (Fig. 1D) as the point of contact using a small amount of (Loctite) super glue applied to the bee with a pipette tip. As when using normal queen marking plates, the marker was positioned in the center front of the thorax, and care was taken to not apply glue to or otherwise obstruct the bee's wings. Marked bees were then transported to Falcon tubes (with air holes) for release. Bee markers weighed 20 mg (range of 16 to 28 mg; mean average of 18 markers).

Statistical analysis

All data collected to estimate absolute tracking accuracy and precision with this FLO system were used, with no removal of outliers or other values (Fig. 3F). For offline distance estimates from the quadcopter, 49.5 s of data (from a total of 260 s) were masked (censored) by manual outlier removal (Fig. 4 and Movie 2). Comparing simultaneously captured video from the infrared tracking camera used by FLO, video from the pilot's goggle view, and the raw distance estimate values revealed that most of these outliers could be attributed to specular reflections from the device used by an experimenter to encourage bee flight.

Supplementary Materials

The PDF file includes:

Legends for movies S1 to S5

Legend for data file S1

Other Supplementary Material for this manuscript includes the following:
Movies S1 to S5
Data file S1
MDAR Reproducibility Checklist

REFERENCES AND NOTES

1. A.-M. Klein, B. E. Vaissière, J. H. Cane, I. Steffan-Dewenter, S. A. Cunningham, C. Kremen, T. Tscharntke, Importance of pollinators in changing landscapes for world crops. *Proc. R. Soc. B: Biol. Sci.* **274**, 303–313 (2007).
2. D. L. Wagner, E. M. Grames, M. L. Forister, M. R. Berenbaum, D. Stopak, Insect decline in the anthropocene: Death by a thousand cuts. *Proc. Natl. Acad. Sci. U.S.A.* **118**, e2023989118 (2021).
3. K. von Frisch, *The Dance Language and Orientation of Bees* (Harvard Univ. Press, 1967).
4. J. R. Riley, A. D. Smith, D. R. Reynolds, A. S. Edwards, J. L. Osborne, I. H. Williams, N. L. Carreck, G. M. Poppy, Tracking bees with harmonic radar. *Nature* **379**, 29–30 (1996).
5. V. A. Drake, D. R. Reynolds, *Radar Entomology: Observing Insect Flight and Migration* (CABI Publishing, 2012).
6. J. L. Woodgate, J. C. Makinson, K. S. Lim, A. M. Reynolds, L. Chittka, Life-long radar tracking of bumblebees. *PLOS ONE* **11**, e0160333 (2016).
7. M. Mischiati, H.-T. Lin, P. Herold, E. Imler, R. Olberg, A. Leonardo, Internal models direct dragonfly interception steering. *Nature* **517**, 333–338 (2015).
8. P. Goyal, A. Cribellier, G. C. H. E. de Croon, M. J. Lankheet, J. L. van Leeuwen, R. P. M. Pieters, F. T. Muijres, Bumblebees land rapidly and robustly using a sophisticated modular flight control strategy. *iScience* **24**, 102407 (2021).
9. A. D. Straw, Review of methods for animal videography using camera systems that automatically move to follow the animal. *Integr. Comp. Biol.* **61**, 917–925 (2021).
10. E. de Margerie, M. Simonneau, J.-P. Caudal, C. Houdelier, S. Lumineau, 3D tracking of animals in the field using rotational stereo videography. *J. Exp. Biol.* **218**, 2496–2504 (2015).
11. H. C. Berg, How to track bacteria. *Rev. Sci. Instrum.* **42**, 868–871 (1971).
12. N. Ogawa, H. Oku, K. Hashimoto, M. Ishikawa, Microrobotic visual control of motile cells using high-speed tracking system. *IEEE Trans. Robot.* **21**, 704–712 (2005).
13. S. Faumont, G. Rondeau, T. R. Thiele, K. J. Lawton, K. E. McCormick, M. Sottile, O. Griesbeck, E. S. Hecksher, W. M. Roberts, C. Q. Doe, S. R. Lockery, An image-free opto-mechanical system for creating virtual environments and imaging neuronal activity in freely moving *Caenorhabditis elegans*. *PLOS ONE* **6**, e24666 (2011).
14. K. Okumura, H. Oku, M. Ishikawa, "High-speed gaze controller for millisecond-order pan/tilt camera" in *2011 IEEE International Conference on Robotics and Automation* (IEEE, 2011), pp. 6186–6191.
15. T. Hatori, J. Hirota, J. Sakakibara, Automatic optical tracking of a flying bird. *Trans. Vis. Soc. Japan* **36**, 1–7 (2016).
16. N. Fujiwara, M. Jiang, T. Takaki, I. Ishii, K. Shimasaki, "Super-telephoto drone tracking using HFR-video-based vibration source localization" in *2019 IEEE International Conference on Robotics and Biomimetics (ROBIO)* (IEEE, 2019), pp. 2239–2244.
17. J. Sakakibara, J. Kita, N. Osato, Note: High-speed optical tracking of a flying insect. *Rev. Sci. Instrum.* **83**, 036103 (2012).
18. R. Pannequin, M. Jouaiti, M. Boutayeb, P. Lucas, D. Martinez, Automatic tracking of free-flying insects using a cable-driven robot. *Sci. Robot.* **5**, eabb2890 (2020).
19. T. Walter, J. Degen, K. Pfeiffer, A. Stöckl, S. Montenegro, T. Degen, A new innovative real-time tracking method for flying insects applicable under natural conditions. *BMC Zool.* **6**, 35 (2021).
20. B. D. Rennison, W. H. R. Lumsden, C. J. Webb, Use of reflecting paints for locating tsetse fly at night. *Nature* **181**, 1354–1355 (1958).
21. P. O. Zanen, R. T. Cardé, Directional control by male gypsy moths of upwind flight along a pheromone plume in three wind speeds. *J. Comp. Physiol. A* **184**, 21–35 (1999).
22. M. T. Smith, M. Livingstone, R. Comont, A method for low-cost, low-impact insect tracking using retroreflective tags. *Methods Ecol. Evol.* **12**, 2184–2195 (2021).
23. T. T. Vo-Doan, A. D. Straw, Millisecond insect tracking system. arXiv:2002.12100 [q-bio.QM] (2020).
24. D. E. Bath, J. R. Stowers, D. Hörmann, A. Poehlmann, B. J. Dickson, A. D. Straw, FlyMAD: Rapid thermogenetic control of neuronal activity in freely walking *Drosophila*. *Nat. Methods* **11**, 756–762 (2014).
25. A. Nourizonoz, R. Zimmermann, C. L. A. Ho, S. Pellat, Y. Ormen, C. Prévost-Solié, G. Reymond, F. Pifferi, F. Aujard, A. Herrel, D. Huber, EthoLoop: Automated closed-loop neuroethology in naturalistic environments. *Nat. Methods* **17**, 1052–1059 (2020).
26. D. Goulson, J. Peat, J. C. Stout, J. Tucker, B. Darvill, L. C. Derwent, W. O. H. Hughes, Can alloethism in workers of the bumblebee, *Bombus terrestris*, be explained in terms of foraging efficiency? *Anim. Behav.* **64**, 123–130 (2002).
27. T. J. Wolf, P. Schmid-Hempel, Extra loads and foraging life span in honeybee workers. *J. Anim. Ecol.* **58**, 943–954 (1989).
28. J. Redmon, S. Divvala, R. Girshick, A. Farhadi, "You only look once: Unified, real-time object detection" in *Proceedings of the IEEE Conference on Computer Vision and Pattern Recognition (CVPR)* (IEEE, 2016), pp. 779–788.
29. E. Gebauer, S. Thiele, P. Ouvrard, A. Sicard, B. Risse, "Towards a dynamic vision sensor-based insect camera trap" in *Proceedings of the IEEE/CVF Winter Conference on Applications of Computer Vision (WACV)* (IEEE, 2024), pp. 7157–7166.

Acknowledgments: We thank M. Siegel and the mechanical workshop of the Institute of Biology I for constant assistance, M. Wittlinger for use of the high-speed video camera, J. Klein for assistance with bee experiments, E. Wagner for use of the field used in the drone experiments, and N. Brehm and M. Böhler for beekeeping. **Funding:** This work was funded by an HFSP cross-disciplinary fellowship (LT000221/2019-C to T.T.V.-D.) and the VolkswagenFoundation Momentum Program (AZ 98692 to A.D.S.). **Author contributions:** Conceptualization: T.T.V.-D. and A.D.S. Funding acquisition: T.T.V.-D. and A.D.S. Investigation: T.T.V.-D., V.V.T., M.J.M.H., S.L., and A.D.S. Methodology: T.T.V.-D., V.V.T., M.J.M.H., S.L., and A.D.S. Project administration: A.D.S. Software: V.V.T., S.L., and A.D.S. Supervision: A.D.S. Visualization: T.T.V.-D. and A.D.S. Writing—original draft: A.D.S. Writing—review and editing: T.T.V.-D., V.V.T., M.J.M.H., S.L., and A.D.S. **Competing interests:** The authors declare that they have no competing interests. **Data and materials availability:** FLO controller software: https://doi.org/10.5281/zenodo.13757151. Hardware design files and build instructions: https://doi.org/10.5281/zenodo.13757197. Analysis software: https://doi.org/10.5281/zenodo.13757080. Data: https://doi.org/10.5061/dryad.bvq83bkjr.

Submitted 7 November 2023
Accepted 18 September 2024
Published 16 October 2024
10.1126/scirobotics.adm7689

Science Robotics

High-resolution outdoor videography of insects using Fast Lock-On tracking

T. Thang Vo-Doan, Victor V. Titov, Michael J. M. Harrap, Stephan Lochner, and Andrew D. Straw

Sci. Robot. **9** (95), eadm7689. DOI: 10.1126/scirobotics.adm7689

Editor's summary

Studying insects in their natural environments can provide important insight into their behavior. However, videography of flying insects, especially outdoors, is difficult because of their small size and fast motion. After tagging an insect with a distinct marker, Vo-Doan *et al*. developed a system called Fast Lock-On (FLO) tracking that uses a feedback system to tilt the camera's mirror position and keep the insect in focus. Using FLO, high-speed, high-resolution videos of a honey bee and locust were successfully captured with low motion blur. The FLO system was then incorporated onto a drone enabling video collection of a marked honey bee for several minutes, unlocking the potential for tracking insects on the kilometer scale. —Melisa Yashinski

Science Robotics (ISSN 2470-9476) is published by the American Association for the Advancement of Science. 1200 New York Avenue NW, Washington, DC 20005. The title *Science Robotics* is a registered trademark of AAAS.